Cite this: DOI: 10.1039/c0xx00000x

www.rsc.org/xxxxxx

ARTICLE

Decomposition of nitroimidazole ions: experiment and theory

Linda Feketeová,[*a,b] **Johannes Postler,**[c] **Athanasios Zavras,**[a] **Paul Scheier,**[c] **Stephan Denifl**[c] **and Richard A. J. O'Hair**[a]

Received (in XXX, XXX) Xth XXXXXXXXX 20XX, Accepted Xth XXXXXXXXX 20XX
DOI: 10.1039/b000000x

Nitroimidazoles are important compounds with chemotherapeutic applications as antibacterial drugs or as radiosensitizers in radiotherapy. Despite their use in biological applications, little is known about the fundamental properties of these compounds. Understanding the ionization reactions of these compounds is crucial in evaluating the radiosensitization potential and in developing new and more effective drugs. Thus, the present study investigates the decomposition of negative and positive ions of 2-nitroimidazole and 4(5)-nitroimidazole using low- and high-energy Collision-Induced Dissociation (CID) and Electron-Induced Dissociation (EID) by two different mass spectrometry techniques and is supported by quantum chemistry calculations. EID of $[M+H]^+$ leads to more extensive fragmentation than CID and involves many radical cleavages including loss of $H^•$ leading to the formation of the radical cation, $M^{•+}$. The stability (metastable decay) and the fragmentation (high-energy CID) of the radical cation $M^{•+}$ have been probed in a crossed-beam experiment involving primary electron ionization of the neutral nitroimidazole. Thus, fragments in the EID spectra of $[M+H]^+$ that come from further dissociation of radical cation $M^{•+}$ has been highlighted. The loss of $NO^•$ radical from $M^{•+}$ is associated with a high Kinetic Energy Release (KER) of 0.98 eV. EID of $[M-H]^-$ also leads to additional fragments compared to CID, however, with much lower cross section. Only EID of $[M+H]^+$ leads to a slight difference in the decomposition of 2-nitroimidazole and 4(5)-nitroimidazole.

1. Introduction

Nitroimidazolic compounds play an important role in chemotherapeutic applications due to their well-known antibacterial activity[1,2] and more recently due to their successful use as radiosensitizers in radiation therapy,[3,4] as well as their emerging application as agents for imaging hypoxia in tumours by positron emission tomography (PET).[5,6] Additionally, nitroimidazolic compounds have attracted interest due to their potential use as energetic materials, such as, explosives or propellants[7-9] due to the presence of the $-NO_2$ nitro functional group known as 'explosophore'. Despite being employed in chemotherapeutic applications, little is known about their fundamental properties, which becomes even more crucial due to the potential ecotoxicity through bioaccumulation in hospital sewage water.[10-12]

Gas-phase studies of nitroimidazoles are limited to the pioneering photoelectron spectroscopy (PES) work by Kajfež et al. on 4(5)-nitroimidazole and methyl-nitroimidazoles,[13] followed by a PES and mass analyzed kinetic energy spectra (MIKE) study of 4(5)-nitroimidazole by Jimenez et al.,[14] and a recent nanosecond energy resolved spectroscopy study by Yu.[7,8] Recently, the first mass spectrometry study on nitroimidazolic radiosensitizers and related nitroimidazolic compounds investigated the formation of radical anions, which is believed to be a key step in the radiosensitization.[15] Subsequently Tanzer et al. showed that methylation of nitroimidazole at the N1 site completely blocks the rich chemistry induced by the attachment of low energy (< 2 eV) free electrons.[16] These reports highlight the importance of fundamental knowledge of the physical and chemical properties of these compounds in order to progress applications of nitroimidazoles as radiosensitizers in tumour radiation therapy or as future explosive materials. The present study adds to this fundamental knowledge by focusing on the fragmentation of negative and positive ions of 2-nitroimidazole and 4(5)-nitroimidazole (Figure 1) using low- and high-energy Collision-Induced Dissociation (CID) and Electron-Induced Dissociation (EID) by two different mass spectrometry techniques in conjunction with the use of DFT calculations.

While low-energy CID (usually in a sub-eV range) that requires multiple collisions, thus termed a 'slow heating' process, leads to the dissociation of the ion through vibrational excitation, high-energy CID (in a keV range) and EID (> 20 eV) involve a single collision leading to an electronically excited state of the ion as well as possible coupling to its vibrational states. Thus, the combination of these techniques can give complementary structural information on gas-phase ions.

2. Methods

2.1 Materials

2-nitroimidazole (**1**) and 4-nitroimidazole (**2a**), which is a regioisomer of 5-nitroimidazole (**2b**) (see Figure 1), were purchased from Aldrich (98%) and Alfa Aesar (97%), respectively. 4-nitroimidazole (**2a**) and 5-nitroimidazole (**2b**) are annular tautomers that differ in the position of H atom on either of the two N atoms within the nitroimidazole ring. The tautomeric equilibrium favors 4-nitroimidazole in the crystal structure. 5-nitroimidazole is most stable in the gas phase,[17] however, both tautomers have been recently observed in the gas phase at nearly equal levels.[18] N-protonation or deprotonation of 4-nitroimidazole and 5-nitroimidazole leads to the formation of identical $[M+H]^+$ and $[M-H]^-$, respectively (Figure 1).

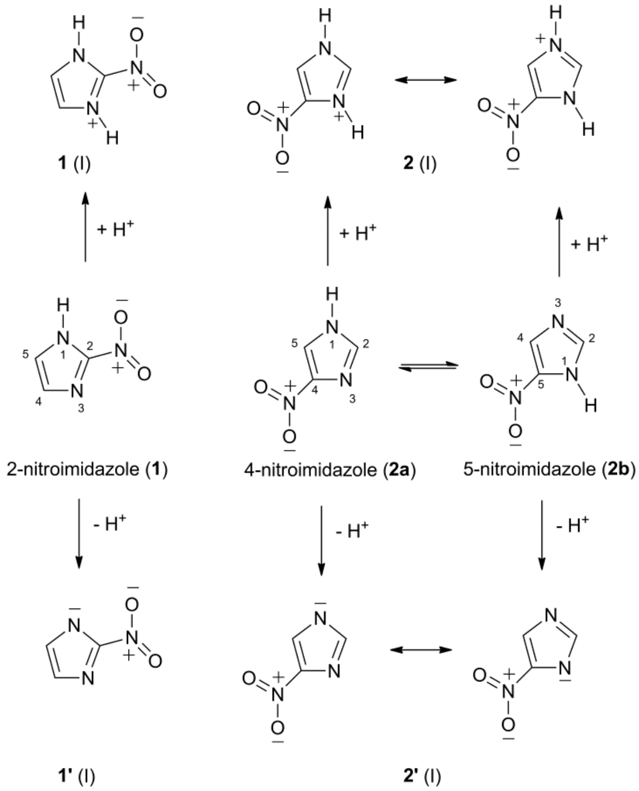

Fig. 1 Structures of nitroimidazole compounds investigated: 2-nitroimidazole (**1**), 4-nitroimidazole (**2a**), 5-nitroimidazole (**2b**). **2a** and **2b** are annular tautomers which produce the same $[M+H]^+$ and $[M-H]^-$ upon N-protonation or N-deprotonation respectively.

2.2 Ion trap LTQ-FT mass spectrometry (low-energy CID)

All experiments were carried out on a Finnigan- LTQ-FT (Thermo, Bremen, Germany) mass spectrometer equipped with an electrospray ionization (ESI) source[19,20] described in detail elsewhere.[21,22] Samples were dissolved in methanol and then introduced to ESI source of the mass spectrometer via direct infusion using the factory supplied syringe pump operating at a flow rate of 5.0 µL/min. Typical ESI conditions used were: spray voltage, 3.0 - 5.0 kV, capillary temperature, 250 - 330 ^{o}C, nitrogen sheath pressure, 5 - 30 (arbitrary units). The capillary voltage and the tube lens offset were tuned to maximize the desired peak. The injection time was set using the automatic gain control function. The LTQ-FT mass spectrometer consists of: (i) Linear ion Trap (LTQ); (ii) ion transfer optics; and (iii) FT-ICR mass analyzer. For the tandem mass spectrometry experiments, the desired ions produced via ESI were mass selected, trapped in the LTQ and subjected to CID at a He bath gas pressure of ca. 5 x 10^{-3} Torr. CID was carried out by mass selecting the desired ions with a 1.8 *m/z* units window and subjecting them to the following typical conditions: normalized collision energy 40 % (RF amplitude, 100 % = 5 V), activation (Q) 0.25, and activation time of 30 ms. In order to minimize background noise, the CID conditions used for $[M+H]^+$ of 4(5)-nitroimidazole were: selection window of 1.5 *m/z*, normalized collision energy 50 % and activation time of 1 ms. For high-resolution mass analysis, the ions were transferred via the ion optics transfer region (~ 2 x 10^{-7} Torr) into an FT-ICR cell at a pressure below 1.5 x 10^{-9} Torr.

The FT-ICR cell is supplied with low energy electrons produced by an indirectly heated emitter cathode located downstream of the FT-ICR cell. The energy of electrons is given by the potential difference between the emitter cathode with *ECD offset* of -4.2 V and the grid positioned in front of the cathode, which is variable. Ions were bombarded with 21 – 31 eV electrons at current of 0.03 mA for 30 ms.

2.3 Double focusing mass spectrometry (high-energy CID)

The high energy CID scans have been carried out on a commercial double-focusing 2-sector-field mass spectrometer (VG ZAB2-SEQ) in reverse Nier-Johnson geometry.[23] Ions were produced by electron bombardment at incident energies of about 70 eV for cation measurements and at low (~ 1.5 eV) energies for anion measurements. The nitroimidazole sample was purchased from Sigma Aldrich (stated purity of 97%) and was heated in an oven to typical temperatures between 360 K and 375 K. The oven was directly placed in front of the ion source in the ion source chamber. Subsequently, the ions were accelerated to 6 keV, momentum-selected by the magnetic sector and subjected to collisions with either ambient air or helium (99.9999%) at variable pressure in the field free region. The resulting ions were energy-selected by the electric sector and detected by a channel electron multiplier (Dr. Sjuts, Germany).

Without introducing air or helium in the field free region the metastable decay of the parent cation was investigated. For the two most abundant product ions we calculated the Kinetic Energy Release (KER) of the reaction by the following formula:

$$KER = \frac{y^2 m_1^2 eV}{16 x m_2 m_3} \left(\frac{\Delta E}{E}\right)^2 \qquad (1)$$

Where m_1 denotes the mass of the parent and m_2 and m_3 respectively the masses of the fragments. The charges of the fragments (in our case 1) are denoted by x and y and V is the acceleration voltage (6 kV). E is the corresponding electric sector voltage and in the case of a Gaussian peak shape ΔE is the width of the peak in the MIKE scan (of which the width of the parent beam has to be substracted). See reference 24 for further details.

2.4 Molecular modelling

Geometries of nitroimidazoles were optimized at the M062x/6-311+G(d,p) level of theory[25-27] with the Gaussian-09B01 program package.[28] Frequencies were calculated to confirm that the structures are local minima on the potential energy surface and not transition states. All energies were corrected for zero-point energies. Transition states (TS) for fragmentation pathways were optimised at the same level of theory and basis set. The frequencies of TS were calculated to confirm that the structures are transition states, i.e., local maxima on the potential energy surface. Calculations of the intrinsic reaction coordinates (IRC) connected the TS to reactants and products.

3. Results and Discussion

3.1 Low-energy CID of $[M+H]^+$

The highest Proton Affinity (PA) for the nitroimidazoles is on the nitrogen of the imidazole ring as opposed to protonation on the oxygen of the NO_2 group (Figure 2). Even though the PA of

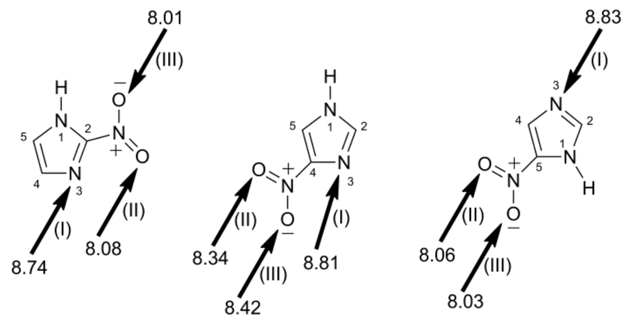

Fig. 2 M062x/6-311+G(d,p) calculated proton affinities for each possible protonation site shown in eV.

4-nitroimidazole (8.81 eV) and 5-nitroimidazole (8.83 eV) are slightly different, the protonation leads to identical $[M+H]^+$ ions as can be seen in Figure 1. CID of $[M+H]^+$ ions of 2-nitroimidazole and 4(5)-nitroimidazole is shown in Figure 3a and 3b, respectively. The three dissociation channels observed for both nitroimidazoles are the loss of the radicals $NO^•$ (Eq. 2) and $NO_2^•$ (Eq. 3) and the loss of H_2O (Eq. 4). The energies required for these dissociation channels are summarized in Table 1, Table 2 and Figure 4.

$$[M+H]^+ \rightarrow C_3H_4N_2O^{•+} + NO^• \quad (2)$$
$$\rightarrow C_3H_4N_2^{•+} + NO_2^• \quad (3)$$
$$\rightarrow C_3H_2N_3O^+ + H_2O \quad (4)$$

The CID spectra of 2-nitroimidazole and 4(5)-nitroimidazole vary in the relative abundance of the formed fragments. While for the 2-nitroimidazole (Figure 3a) the dominant dissociation channel is loss of H_2O (Eq. 4), for the 4(5)-nitroimidazole it is the loss of $NO_2^•$ (Eq. 3, Figure 3b). The loss of $NO_2^•$ requires C–N bond cleavage while the loss of $NO^•$ involves TS of nitro-nitrite isomerisation that leads to immediate loss of $NO^•$ (see Figure 4). The loss of $NO^•$ is an exothermic reaction by 0.45 eV for 2-nitroimidazole but not for 4(5)-nitroimidazole (+0.01 eV).

The loss of H_2O from 2-nitroimidazole requires 2.79 eV (see Table 2 and Figure 4) that involves 3 TS: transfer of H from N1 to the NO_2 group, rotation of the NO_2H, and transfer of the second H from N3 to the OH of the NO_2H. While the energy required for this dissociation channel is comparable to the loss of $NO^•$ of 2.41 eV and loss of $NO_2^•$ of 2.76 eV, it is much lower than the energy required for the loss of H_2O in the case of 4(5)-nitroimidazole of 3.84 eV. The spectrum of 2-nitroimidazole may suggest the protonation to be on the oxygen of the NO_2 group,

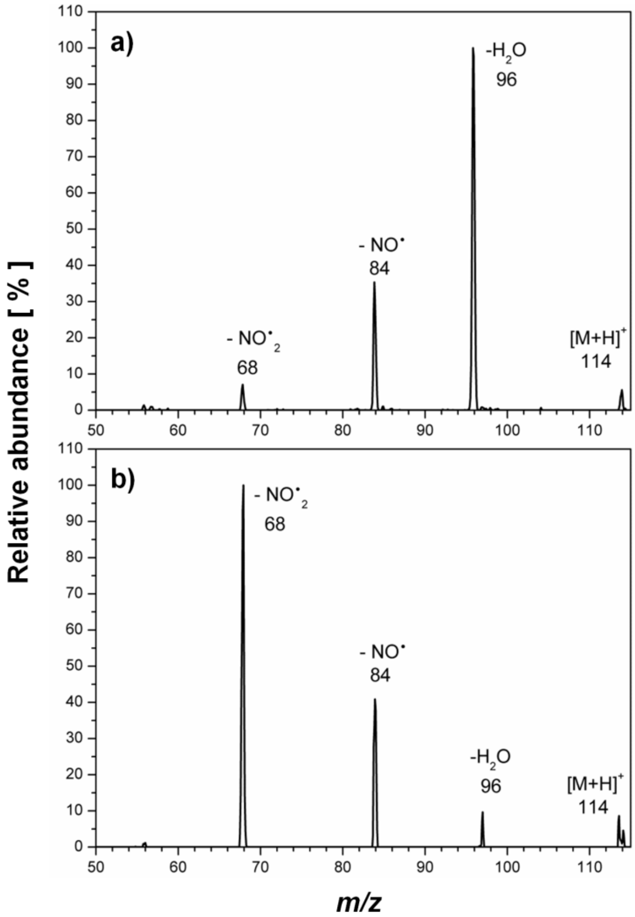

Fig. 3 LTQ-FT low-energy CID spectra of ESI generated $[M+H]^+$ of (a) 2-nitroimidazole and (b) 4(5)-nitroimidazole.

however the PA on this oxygen is 0.73 - 0.7 eV lower than on the N3. Cert et al. suggested protonation of 1-methyl-5-nitroimidazole on the NO_2 group due to the observed loss of H_2O from the respective $[M+H]^+$ ion, however this was not the case for 4(5)-nitroimidazole.[29] The possible explanation for the observed high abundance of the decomposition channel leading to the loss of H_2O in the case of 2-nitroimidazole (Figure 3a) is due to the intrinsic nature of low-energy CID, where ion activation occurs via multiple, discrete, low-energy collisions and thus leads to 'slow heating' of the ion. Thus, due to the low energy barrier for proton transfer $\mathbf{TS_1}_{\text{(I-II)}}$ of 1.03 eV and the rotation of the NO_2H $\mathbf{TS_1}_{\text{(II-III)}}$ of 1.73 eV may lead to an increased population of ions in **1** (III) (see Figure 4a) which will facilitate the decomposition reaction to proceed through loss of H_2O with decreased barrier of 1.73 eV. This is not the same case for 4(5)-nitroimidazole (Figure 4b), where the barrier from the respective $[M+H]^+$ ion in **2** (IV) for the loss of H_2O is still quite high with 2.96 eV. We have also considered the loss of $NO^•$ from 2-nitroimidazole in **1** (III) (Figure 4a), however, the TS was found to be very high in energy of 3.85 eV relative to starting structure **1** (I).

Cite this: DOI: 10.1039/c0xx00000x

www.rsc.org/xxxxxx

ARTICLE

Table 1 Summary of DFT (M062x/6-311+G(d,p) level of theory) calculated energies in eV for reactions resulting in loss of $NO^{\bullet}$ (transition state / sum of products) and loss of $NO_2^{\bullet}$ (bond dissociation energies) of compounds studied.

Parent ion	Neutral loss	Reaction	2-nitroimidazole	4-nitroimidazole	5-nitroimidazole
$[M+H]^+$		(1)	2.41 / -0.45	2.75 / 0.01	2.75 / 0.01
$M^{\bullet+}$	$NO^{\bullet}$	(7)	1.24 / -1.54	1.22 / -1.19	1.36 / -1.58
$[M-H]^-$		(11)	2.87 / 0.48	3.03 / 0.61	3.03 / 0.61
$[M+H]^+$		(3)	2.76	2.89	2.89
$M^{\bullet+}$	$NO_2^{\bullet}$	(9)	2.97	2.68	3.08
$[M-H]^-$		(13)	4.03	4.21	4.21

Table 2 Summary of DFT (M062x/6-311+G(d,p) level of theory) calculated energies in eV for further dissociation reactions of compounds studied.

Parent ion	Neutral loss	Reaction	2-nitroimidazole	4-nitroimidazole	5-nitroimidazole
$[M+H]^+$	H_2O	(4)[a]	2.79	3.84	3.84
$[M+H]^+$	$H^{\bullet}$	(5)	5.01	5.08	5.21
$M^{\bullet+}$	$NO^{\bullet}$ + CO	(8)[b]	-0.77[c]	(2.56) 1.37 / 0.99	(1.27) -0.31 / -0.68
$M^{\bullet+}$	O	(6)	5.00	4.74	4.88
$M^{\bullet+}$	O + $NO^{\bullet}$	(10)	8.44	8.15	8.55
$[M-H]^-$	O	(12)	6.45	6.46	6.46
$[M-H]^-$	O + $NO^{\bullet}$		9.50	9.69	9.69

[a] Loss of H_2O involves 3 (2-nitroimidazole) - 4 (4- and 5-nitroimidazole) transition states, values given are the sum of formed products.

[b] This dissociation channel is a consecutive loss of $NO^{\bullet}$ and then CO, thus values for 4-nitroimidazole and 5-nitroimidazole present energies of transition states relative to ($[M-NO]^+$) $M^{\bullet+}$ respectively, and the sum of energies of the products.

[c] The fragment ion $C_2H_3N_2^+$ has not been observed in the EID of protonated 2-nitroimidazole in comparison to 4(5)-nitroimidazole. The transition state for the loss of CO lead to dissociation into more than 2 fragments. The value given is a sum of energies of the products.

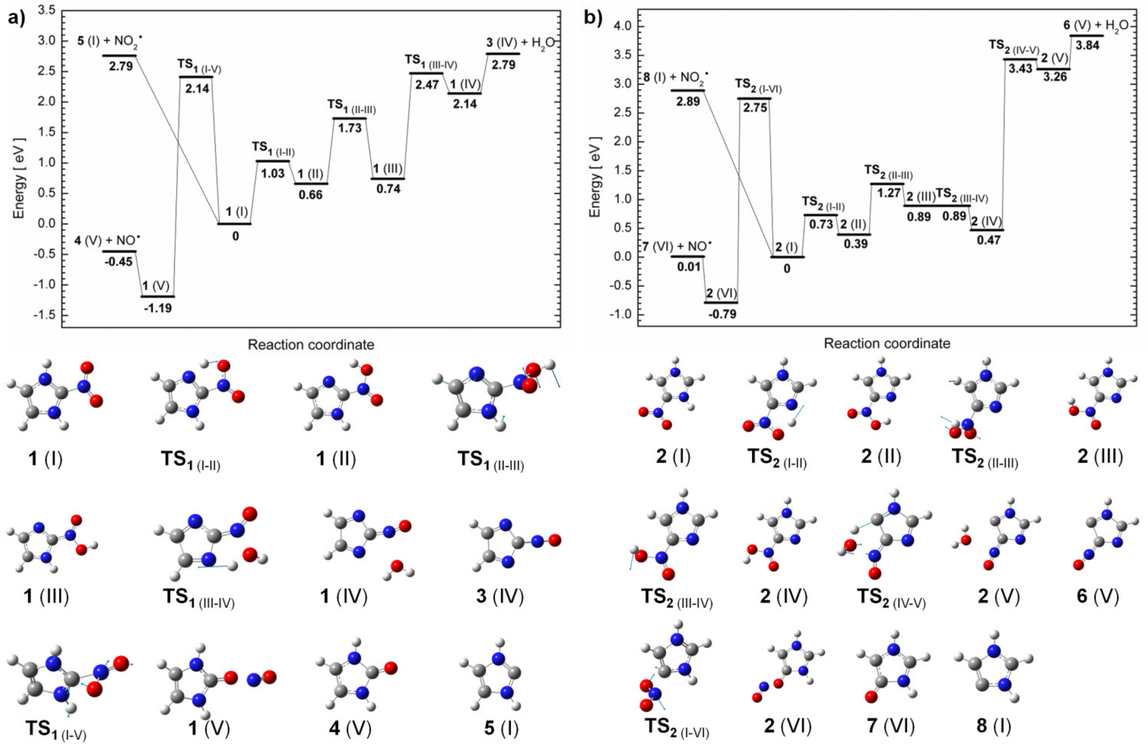

Fig. 4 M062x/6-311+G(d,p) calculated potential energy diagram for decomposition of the $[M+H]^+$ ion, where M = (a) 2-nitroimidazole and (b) 4(5)-nitroimidazole. Calculated energy values in eV include a zero-point energy correction. The blue arrows in the respective TS show the displacement vectors.

Cite this: DOI: 10.1039/c0xx00000x

www.rsc.org/xxxxxx

ARTICLE

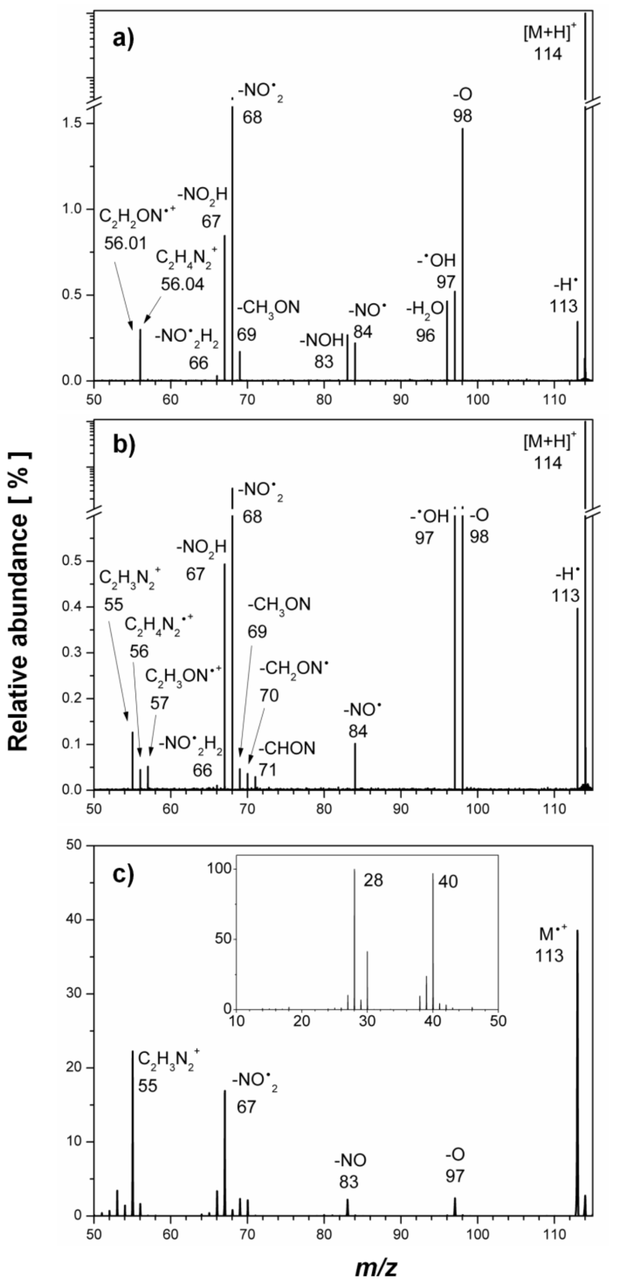

Fig. 5 LTQ-FT EID spectra of ESI generated $[M+H]^+$ of (a) 2-nitroimidazole and (b) 4(5)-nitroimidazole at electron energy of 21 eV; and (c) VG ZAB2-SEQ electron ionization mass spectrum of 4(5)-nitroimidazole with an electron energy of ~70eV.

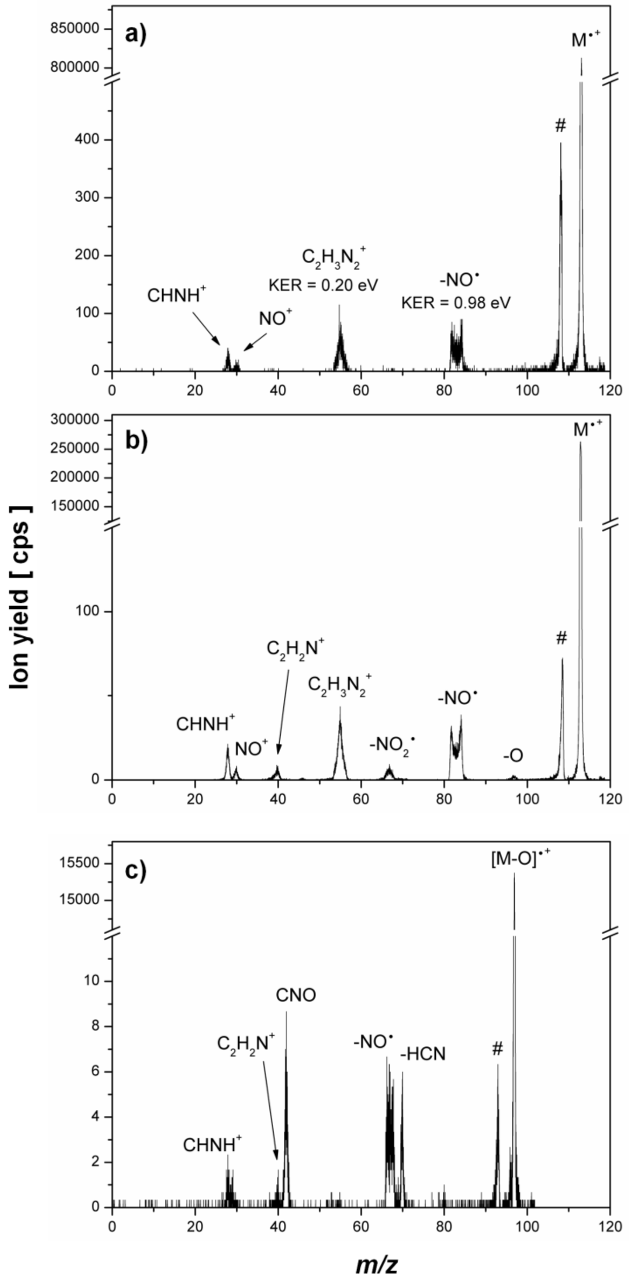

Fig. 6 VG ZAB2-SEQ tandem mass spectra of cations of 4(5)-nitroimidazole formed via electron ionization (Figure 3c): (a) MIKE scan of $M^{•+}$, and high-energy CID at 6 keV with Helium of (b) $M^{•+}$ and (c) $[M–O]^{•+}$. # is an artefact.

3.2 EID of $[M+H]^+$

EID of 2-nitroimidazole and 4(5)-nitroimidazole is shown in Figure 5a and 5b, respectively. The Figure 5c shows the electron ionization mass spectrum of 4(5)-nitroimidazole (recorded on the VG ZAB2-SEQ at an electron energy of ~70 eV) for comparison. The EID spectra show more extensive fragmentation than the low-energy CID spectra shown in Figure 3, with a number of new channels being observed as discussed below. Notably, the spectra differ for the 2-nitroimidazole and 4(5)-nitromidazole. For both compounds, the loss of $H^•$ radical is observed forming the radical cation $M^{•+}$ (Eq. 5).

$$[M+H]^+ \rightarrow M^{•+} + H^• \qquad (5)$$

The loss of $H^{\bullet}$ radical requires > 5.01 eV, see Table 2. The loss of the $H^{\bullet}$ radical in the EID of protonated ions has been observed earlier for aromatic amino acids and has been suggested to take place through an electronically excited state of the aromatic side chain that couples to the dissociative state.[30] The resultant radical cation $M^{\bullet+}$ is likely to be formed in an excited state and can thus undergo further fragmentation.[30,31] As a consequence, the EID spectra closely resemble the electron ionization spectrum with characteristic losses of O, $NO^{\bullet}$ and $NO_2^{\bullet}$. Thus, in the EID of 2-nitroimidazole (Figure 5a) the loss of O forming an ion at *m/z* 98 comes from the dissociation of $[M+H]^+$, while the fragment ion at *m/z* 97 originates from the dissociation of $M^{\bullet+}$ (Eq. 6). Similarly, the loss of $NO^{\bullet}$ from the protonated parent ion forms a fragment at *m/z* 84 (Eq. 2), while the loss of $NO^{\bullet}$ from the radical cation forms a fragment ion at *m/z* 83 (Eq. 7). The loss of $NO_2^{\bullet}$ from $[M+H]^+$ and $M^{\bullet+}$ leads to fragment ions at *m/z* 68 and 67, respectively. The EID spectrum of 4(5)-nitroimidazole (Figure 5b) appears similar to 2-nitroimidazole, however, there are some notable differences: (i) there is no H_2O loss in the EID of 4(5)-nitroimidazole; (ii) there is no loss of $NO^{\bullet}$ from the radical cation of 4(5)-nitroimidazole; and (iii) the fragment ion $C_2H_3N_2^+$ at *m/z* 55 is observed that is formed from dissociation of the $M^{\bullet+}$ as can be seen from comparison of the electron ionization spectrum in Figure 5c.

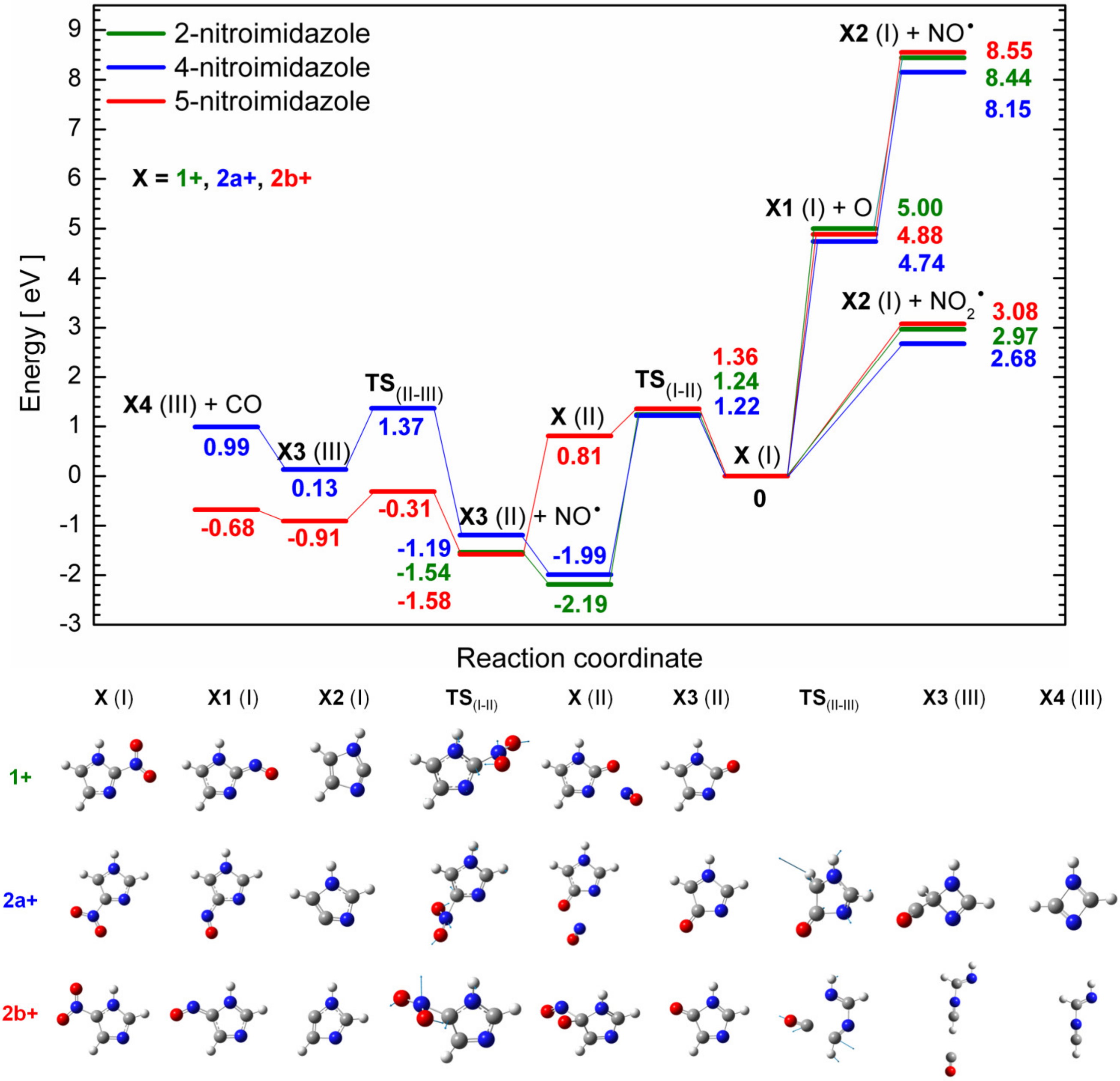

Fig. 7 M062x/6-311+G(d,p) calculated potential energy diagram for decomposition of the $M^{\bullet+}$ radical cation, where M = 2-nitroimidazole (green), 4-nitroimidazole (blue), and 5-nitroimidazole (red). Calculated energy values in eV include a zero-point energy correction. The blue arrows in the respective TS show the displacement vectors.

Cite this: DOI: 10.1039/c0xx00000x
www.rsc.org/xxxxxx

ARTICLE

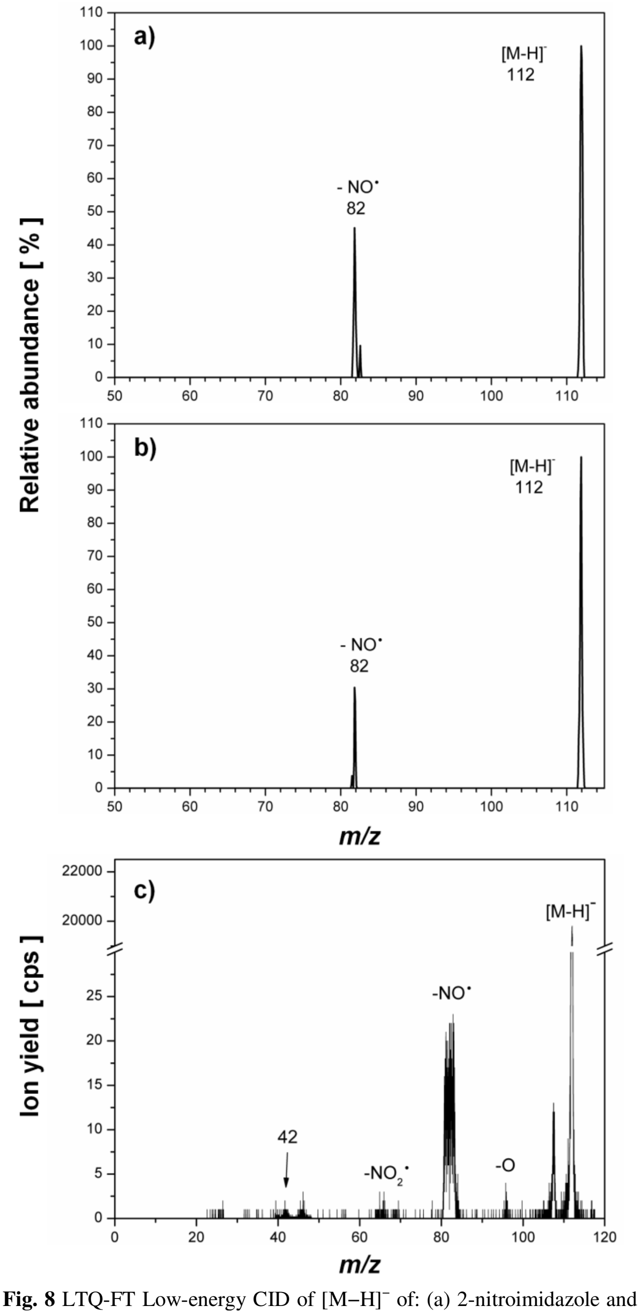

Fig. 8 LTQ-FT Low-energy CID of $[M-H]^-$ of: (a) 2-nitroimidazole and (b) 4(5)-nitroimidazole. Panel (c) shows VG ZAB2-SEQ high-energy CID of $[M-H]^-$ of 4(5)-nitroimidazole in air.

3.3 Metastable decay and high-energy CID of $M^{•+}$

Figure 6 shows the MIKE spectrum of metastable $M^{•+}$ of 4(5)-nitroimidazole (Figure 6a) and high-energy CID spectra of $M^{•+}$ and $[M-O]^{•+}$ in Figure 6b and 6c, respectively. The metastable decay of the parent radical cation $M^{•+}$ results mainly in loss of $NO^•$ (Eq. 7) and further loss of CO forming fragment ion $C_2H_3N_2^+$ at *m/z* 55 (Eq. 8). The successive loss of $NO^•$ and CO has been proposed by Luijten et al. in the study of the methylated nitroimidazoles.[32] The decay peak of $C_2H_3N_2^+$ has a Gaussian peak shape indicating a rather small KER. Indeed, the calculation of the KER using equation (1) leads to a value of about 200 meV. In contrast, the decay peak for loss of $NO^•$ from the parent cation exhibits a dished peak structure which is present in case of a high KER. Jimenez et al.[14] reported a large KER of about 0.85 eV (determined from the distance of the two "horns" of the dished peak structure). The evaluation based on equation (1) shows a slightly higher KER of 0.98 eV for the loss of $NO^•$, in agreement with the previous work. Such a high KER for a metastable dissociation reaction is characteristic of an explosive reaction and an energetic material as for example previously observed for the TNT precursor dinitrotoluene.[33]

$$
\begin{aligned}
M^{•+} \quad & \rightarrow C_3H_3N_3O^{•+} + O && (6)\\
& \rightarrow C_3H_3N_2O^{+} + NO^{•} && (7)\\
& \rightarrow C_2H_3N_2^{+} + CO + NO^{•} && (8)\\
& \rightarrow C_3H_3N_2^{+} + NO_2^{•} && (9)\\
& \rightarrow C_3H_3N_2^{+} + O + NO^{•} && (10)
\end{aligned}
$$

The high-energy CID of $M^{•+}$ shown in Figure 6b shows several new fragments in comparison to the MIKE scan in Figure 6a, namely, the loss of O (Eq. 6), $NO_2^•$ (Eq. 9), and the formation of fragment ion $C_2H_2N^+$ at *m/z* 40. The CID spectra shown were recorded by introducing helium in the field free region; CID using air led to virtually identical spectra. The high-energy CID of $[M-O]^{•+}$ in Figure 6c reveals that $NO_2^•$ can be lost either directly (Eq. 9) or from successive loss of O and $NO^•$ (Eq. 10). The successive loss has been suggested by Luijten et al.[32] in the mass spectrometry of methylated nitroimidazoles. The same appears to be true for the formation of the fragment ions at *m/z* 40 and 28 that also appear in the CID spectrum of $[M-O]^{•+}$ in Figure 6c. The high-energy CID of radical cation $M^{•+}$ (Figure 6b) closely resembles the EID spectrum of $[M+H]^+$ (Figure 5b) considering the fragmentation pathways of the radical cation $M^{•+}$ formed via EID of $[M+H]^+$ (Eq. 5). Thus, the excitation energy deposited in the high-energy collision is similar to the excitation energy transferred in the collisions with ~ 25 eV electrons. The energies required for the dissociation channels Eqs. 6 - 10 are summarised in Table 1, Table 2 and Figure 7 that includes all structures associated with these channels.

3.4 CID and EID of $[M-H]^-$

The low-energy CID of $[M-H]^-$ for 2-nitroimidazole and 4(5)-nitroimidazole is shown in Figure 8a and 8b, respectively. Only one dissociation pathway is observed due to the loss of $NO^•$ (Eq. 11) forming the radical anion at *m/z* 82. The energy required for the loss of $NO^•$ is summarized in Table 1 and Figure 9 includes the potential energy diagram and structures associated with the loss of $NO^•$. The high-energy CID of the dehydrogenated 4(5)-nitroimidazole anion is shown in Figure 8c.

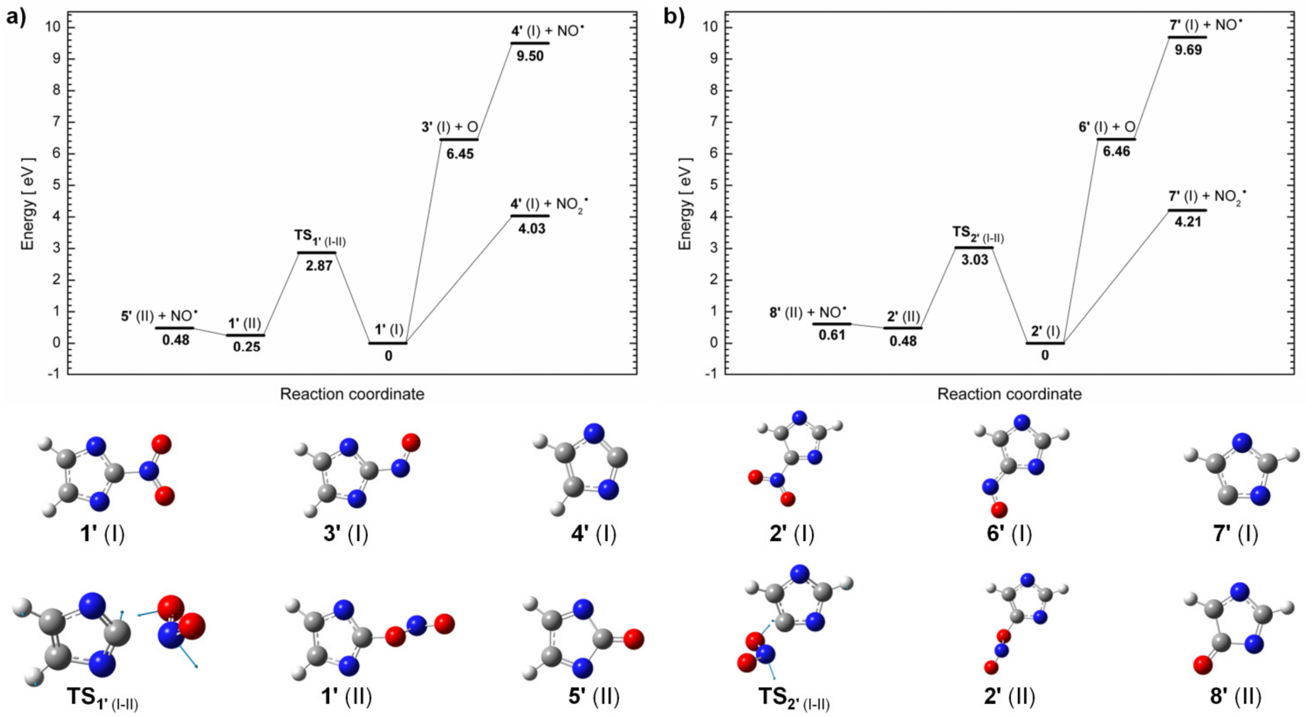

Fig. 9 M062x/6-311+G(d,p) calculated potential energy diagram for decomposition of the $[M-H]^-$ anion, where M = (a) 2-nitroimidazole and (b) 4(5)-nitroimidazole. Calculated energy values in eV include a zero-point energy correction. The blue arrows in the respective TS show the displacement vectors.

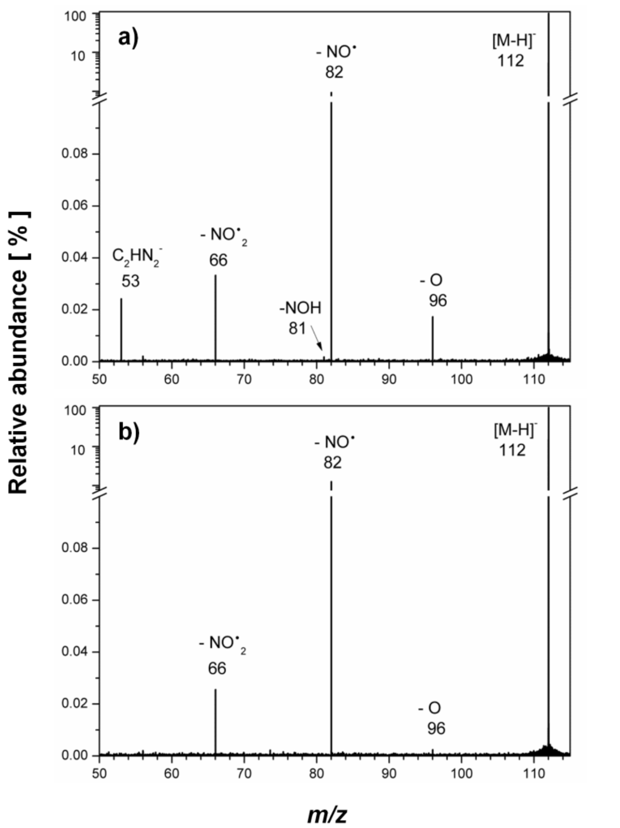

Fig. 10 LTQ-FT EID of ESI generated $[M-H]^-$ of: (a) 2-nitroimidazole at 21 eV electron energy and (b) 4(5)-nitroimidazole at 31 eV electron energy.

Due to the excess of energy in high-energy collision, a number of new fragments like for example the loss of O (Eq. 12) and loss of $NO_2^•$ (Eq. 13) appear in comparison to low-energy CID in Figure 8b well in accordance with calculated energy required for these losses depicted in Figure 9. The high-energy CID agrees with the EID of $[M-H]^-$ of 4(5)-nitroimidazole shown in Figure 10b, where the observed fragments are due to the losses of O, $NO^•$ and $NO_2^•$ (Eqs. 11-13). The EID of $[M-H]^-$ of 2-nitroimidazole shown in Figure 10a in comparison to 4(5)-nitroimidazole leads to two new fragment ions $C_2HN_2^-$ at *m/z* 53 and $C_3HN_2O^-$ at *m/z* 81.

$$[M-H]^- \rightarrow C_3H_2N_2O^{•-} + NO^• \quad (11)$$
$$\rightarrow C_3H_2N_3O^- + O \quad (12)$$
$$\rightarrow C_3H_2N_2^{•-} + NO_2^• \quad (13)$$

3.5 Losses of $NO^•$ and $NO_2^•$

The present results show that irrespective of the nature of the nitroimidazole ions studied, the decomposition of the nitroimidazoles involves nitro functional group $-NO_2$ in all cases. Notably, similar result has been observed in the fragmentation of charged imidacloprid possessing nitro-guanidine functional group $-N-NO_2$ that has been observed to be involved in the dissociation of the charged species.[34] Even though, the dissociation of nitroimidazoles varies depending on the nature of the charge, the decomposition channels present in all cases involve loss of $NO^•$ and $NO_2^•$. Only in the low-energy CID of $[M-H]^-$ (Figure 8) is the loss of $NO_2^•$ absent. The energies required for these losses are summarized in Table 1. The loss of $NO_2^•$ requires the C–N bond cleavage. The strength of this bond is important in evaluating the stability and sensitivity of energetic materials.[8] The bond dissociation energy is highest for the deprotonated anions $[M-H]^-$ requiring > 4.03 eV, which is even higher than the energy required for this loss in the case of neutral compounds ~ 3.5 eV.[7] Likely due to this high bond dissociation energy, and the large energetic difference between the loss of $NO^\bullet$ and $NO_2^\bullet$ of ~1.2 eV (Table 1, Figure 9) and the fact of the 'slow heating' process in low-energy CID, the loss of $NO_2^\bullet$ has not been observed in the low-energy CID of $[M-H]^-$. For the positive ions of nitroimidazoles $M^{\bullet+}$ and $[M+H]^+$ the bond dissociation energy ranges from 2.68 - 3.08 eV. The data in Table 1 show that the bond dissociation energy is slightly lower in the case of NO_2 group bound to C2 (2-nitroimidazole) for even electron ions $[M+H]^+$ and $[M-H]^-$. The decomposition reaction resulting in the loss of $NO_2^\bullet$ for nitroimidazoles is energetically less favoured than in the case of compounds with a nitroguanidine functional group where the $N-NO_2$ bond has been reported to be 1.89 eV and even lower of 1.56 eV when H^+ transfer is involved in the dissociation.[34]

The loss of $NO^\bullet$ involves TS of nitro-nitrite isomerisation with a barrier of up to 3 eV irrespective of the charge state of the nitroimidazoles. The loss of $NO^\bullet$ has been reported to be the major fragmentation channel in the UV decomposition of neutral nitroimidazoles.[7] The barriers for nitro-nitrite isomerisation in neutral 2-nitroimidazole and 4(5)-nitroimidazole have been reported to be 3.36 and 3.93 eV, respectively.[7] Current results are observed in the same energy range (see Table 1) however, the barriers for charged species are in some cases substantially lower compared to the neutral ones. The lowest barrier for this dissociation channel is in the case of radical cations $M^{\bullet+}$ (see Table 1) of 1.22 eV, while the highest barrier is in the case of the anions $[M-H]^-$ of 3.03 eV. In the case of even electron species $[M+H]^+$ and $[M-H]^-$, the barriers are lower for the 2-nitroimidazole in comparison to 4(5)-nitroimidazole.

Conclusions

The decomposition of positive and negative ions of 2-nitroimidazole and 4(5)-nitroimidazole was investigated using low- and high-energy CID and EID, and the interpretation of the experimental data was complemented with quantum chemical calculations. Irrespective of the nature of the charge, the decomposition of the nitroimidazoles involves the nitro functional group $-NO_2$ in all cases, via losses of $NO_2^\bullet$ or $NO^\bullet$. The decomposition and neutral losses vary depending on the charge state of the precursor ion, however, the loss of $NO^\bullet$ through nitro-nitrite isomerisation and the loss of $NO_2^\bullet$ were present in all cases except the low-energy CID of $[M-H]^-$ that has not led to loss of $NO_2^\bullet$.

The EID leads to more extensive fragmentation than low-energy CID and involves radical cleavages including loss of $H^\bullet$ that leads to the formation of radical cation $M^{\bullet+}$. Comparison of the fragment ions observed in the high-energy CID and electron impact ionization spectra to those found in the EID of $[M+H]^+$ suggest that EID proceeds via H loss to form the radical cation $M^{\bullet+}$ in an excited state, which then dissociates further to produce the characteristic losses of O, $NO^\bullet$ and $NO_2^\bullet$. The EID spectra differed for the two compounds studied, 2-nitroimidazole and 4(5)-nitroimidazole.

The metastable decay of $M^{\bullet+}$ was investigated for 4(5)-nitroimidazole and showed a large KER of 0.98 eV for the loss of $NO^\bullet$ and a smaller KER of 200 meV for the successive loss of $NO^\bullet$ and CO. The high KER for a metastable dissociation reaction is characteristic of an explosive reaction and is important for consideration as an energetic material. These results should be taken into account in the development of nitroimidazole based radiosensitizers in tumour radiation therapy to improve the compounds efficacy and reduce potential harmful side effects during and post radiation.

Acknowledgements

LF and RAJO thank the ARC for financial support via the ARC Centre of Excellence in Free Radical Chemistry and Biotechnology. LF thanks the ARC for the award of an APD. We acknowledge: an ARC Lief grant and funding from the Victorian Institute for Chemical Sciences for the purchase of the LTQ-FT mass spectrometer; generous grants of computer time (to LF) from The Melbourne University High Performance Computing cluster Edward. This work was partially supported by the Austrian Science Fund FWF (P22665, P26635).

Notes and references

[a] *ARC Centre of Excellence for Free Radical Chemistry and Biotechnology, School of Chemistry and Bio21 Institute of Molecular Science and Biotechnology, The University of Melbourne, 30 Flemington Road, Victoria 3010, Australia.*
[b] *Université de Lyon, 69003 Lyon, France; CNRS/IN2P3, UMR5822, Institut de Physique Nucléaire de Lyon, 69622 Villeurbanne, France. Tel: +33 4 7243 1259; E-mail: l.feketeova@ipnl.in2p3.fr*
[c] *Institut für Ionenphysik und Angewandte Physik and Center for Molecular Biosciences Innsbruck (CMBI), Leopold Franzens Universität Innsbruck, Technikerstrasse 25, A-6020 Austria.*

1 H.-K.S. Leiros, S. Kozielski-Stuhrmann, U. Kapp, L. Terradot, G.A. Leonard and S.M. McSweeney, *J. Biol. Chem.*, 2004, **279**, 55840.
2 A. Mital, *Sci. Pharm.*, 2009, **77**, 497.
3 J. Overgaard, H.S. Hansen, M. Overgaard, L. Bastholt, A. Berthelsen, L. Specht, B.Lindeløv and K. Jørgensen, *Radiother. Oncol.*, 1998, **46**, 135.
4 J. Overgaard, *Radiother. Oncol.*, 2011, **100**, 22.
5 L. Bentzen, S. Keiding, M.R. Horsman, T. Grönroos, S.B. Hansen and J.Overgaard, *Acta Oncol.*, 2002, **41**, 304.
6 Z. Zha, L. Zhu, Y. Liu, F. Du, H. Gan, J. Qiao and H.F. Kung, *Nucl. Med. Biol.*, 2011, **38**, 501.
7 Z. Yu and E.R. Bernstein, *J. Chem. Phys.*, 2012, **137**, 114303.
8 Z. Yu and E.R. Bernstein, *J. Phys. Chem. A*, 2013, **117**, 1756.
9 K.-H. Hou, C.-M. Ma and Z.-L. Liu, *Chinese Chem. Lett.*, 2014, **25**, 438.
10 P.F. Lanzky and B. Halting-Sørensen, *Chemosphere*, 1997, **35**, 2553.
11 R. Lindberg, P. Jarnheimer, B. Olsen, M. Johansson and M. Tysklind, *Chemosphere*, 2004, **57**, 1479.
12 M. Hernández-Mesa, D. Airado-Rodríguez, C. Cruces-Blanco and A. M. García-Campaña, *J. Chromatogr. A*, 2014, **1341**, 65.
13 F. Kajfež, L. Klasinc and V. Šunjić, *J. Heterocyclic Chem.*, 1979, **16**, 529.
14 P. Jimenez, J. Laynes, R. M. Claramunt, D. Sanz, J. P. Fayet, M. C. Vertut, J. Catalán, J. L. G. de Paz, G. Pfister-Guillouzo, C. Guimon, R. Flammang, A. Maquestiau and J. Elguero, *New. J. Chem.*, 1989, **13**, 151.
15 L. Feketeová, A. L. Albright, B. S. Sørensen, M. R. Horsman, J. White, R.A.J. O'Hair and N. Bassler, *Int. J. Mass Spectrom.*, 2014, **365-366**, 56.

16 K. Tanzer, L. Feketeová, B. Puschnigg, P. Scheier, E. Illenberger and S. Denifl, *Angew. Chem. Int. Ed.*, 2014, **53**, 12240.
17 A. I. Vokin, L. V. Sherstyannikova, I. G. Krivoruchka, T. N. Aksamentova, O. V. Krylova and V. K. Turchaninov, *Russ. J. Gen. Chem.*, 2003, **73**, 1028.
18 L. Feketeová, O. Plekan, M. Goonewardane, M. Ahmed, A. L. Albright, J. White, R. A. J. O'Hair, M. R. Horsman, F. Wang and K. C. Prince, *to be published*.
19 R. Malek, W. Metelmann-Strupat, M. Zeller and H. Muenster, *Am. Biotech. Lab.*, 2005, **23**, 8.
20 S. Horning, R. Malek, A. Wieghaus, M.W. Senko and J.E.P. Syka, *Proc. 51st ASMS Conf. Mass Spectrom. Allied Top.*, Montreal, Canada 2003.
21 L. Feketeová, G.N. Khairallah and R.A.J. O'Hair, *Eur. J. Mass Spectrom.*, 2008, **14**, 107.
22 L. Feketeová, *J. Phys.: Conf. Ser.*, 2012, **373**, 012009.
23 E. Alizadeh, F. Ferreira da Silva, F. Zappa, A. Mauracher, M. Probst, S. Denifl, A. Bacher, T.D. Märk, P. Limao-Vieira and P. Scheier, *Int. J. Mass Spect.*, 2008, **271**, 15.
24 R.G. Cooks, J.H. Beynon, R.M. Caprioli and G.R. Lester, *Metastable Ions*, Amsterdam: Elsevier Scientific Pub. Co. 1973.
25 Y. Zhao and D.G. Truhlar, *Theor. Chem. Acc.*, 2008, **120**, 215.
26 R. Ditchfie, W.J. Hehre and J.A. Pople, *J. Chem. Phys.*, 1971, **54**, 724.
27 W.J. Hehre, L. Radom, P.v.R Schleyer and J.A. Pople, *Ab initio molecular orbital theory*, New York: Wiley 1986.
28 Gaussian 09, Revision B.01, M.J. Frisch, G.W. Trucks, H.B. Schlegel, G.E. Scuseria, M.A. Robb, J.R. Cheeseman, G. Scalmani, V. Barone, B. Mennucci, G.A. Petersson, H. Nakatsuji, M. Caricato, X. Li, H.P. Hratchian, A.F. Izmaylov, J. Bloino, G. Zheng, J.L. Sonnenberg, M. Hada, M. Ehara, K. Toyota, R. Fukuda, J. Hasegawa, M. Ishida, T. Nakajima, Y. Honda, O. Kitao, H. Nakai, T. Vreven, J. A. Montgomery, Jr., J.E. Peralta, F. Ogliaro, M. Bearpark, J. J. Heyd, E. Brothers, K.N. Kudin, V.N. Staroverov, T. Keith, R. Kobayashi, J. Normand, K. Raghavachari, A. Rendell, J.C. Burant, S.S. Iyengar, J. Tomasi, M. Cossi, N. Rega, J.M. Millam, M. Klene, J.E. Knox, J.B. Cross, V. Bakken, C. Adamo, J. Jaramillo, R. Gomperts, R.E. Stratmann, O. Yazyev, A.J. Austin, R. Cammi, C. Pomelli, J.W. Ochterski, R.L. Martin, K. Morokuma, V.G. Zakrzewski, G.A. Voth, P. Salvador, J.J. Dannenberg, S. Dapprich, A.D. Daniels, O. Farkas, J.B. Foresman, J.V. Ortiz, J. Cioslowski and D.J. Fox, Gaussian, Inc., Wallingford CT, 2010.
29 A. Cert, P. Delgado-Cobos and M. T. Pérez-Lanzac, *Org. Mass Spectrom.*, 1986, **21**, 499.
30 H. Lioe and R. A. J. O'Hair, *Anal. Bioanal. Chem.*, 2007, **389**, 1429.
31 L. Feketeová, M. W. Wong and R. A. J. O'Hair, *Eur. Phys. J. D*, 2010, **60**, 11.
32 W. C. M. M. Luijten and J. van Thuijl, *Org. Mass Spectrom.*, 1981, **16**, 199.
33 F. Zappa, M. Beikircher, A. Mauracher, S. Denifl, M. Probst, N. Injan, J. Limtrakul, A. Bacher, O. Echt, T. D. Märk, P. Scheier, T. A. Field, K. Graupner, *ChemPhysChem*, 2008, **9**, 607.
34 W. A. Donald, M. G. Leeming and R. A. J. O'Hair, *Int. J. Mass Spectrom.*, 2012, **316-318**, 91.